**Iraqi Geological Journal**

Journal homepage: https://www.igj-iraq.org

# Engineering Site Investigation inside Basrah City, Southern Iraq using Cross-hole Seismic Refraction Technique (A Case Study)

**Iman M. Jaafar[1], Anmar H. Shalih[2], Amer A. Laftah[3] and Emad H. Al-Khersan[4*]**

[1] Department of Geology, College of Science, University of Basrah, Basrah, Iraq
[2] Department of Construction and Project Management, Mustansiriyah University, Baghdad, Iraq
[3] Department of Applied Geology, College of Science, University of Babylon, Hilla, Iraq
[4] Department of Oil and Gas Engineering, College of Oil and Gas, Basrah University for Oil and Gas, Basrah, Iraq
* **Correspondence**: emad.alkhersan@buog.edu.iq

Received: 21 October 2023

Accepted: 2 February 2024

Published: 31 May 2024

**Abstract**

This project includes cross-borehole seismic survey to determine the compressional and shear wave velocities, elastic moduli, and geotechnical properties of the soil at a hospital's site inside Basrah City, Southern part of Iraq to evaluate the required properties of the soil to design a safe foundation for the construction purposes. Five boreholes were drilled in the study area; two of them were to generate waves and the other three boreholes to receive the waves. Standard Penetration Test in borehole 4 showed the existence of weak soft soil at a 10 to 15 m depth. All boreholes from depths 1-15 m were injected with cement and quick-hardening materials to enhance the consistency of the soil. A few days after injection, compressional and shear wave velocities, and the strength of the soil were increased according to this operation and then after, it was considered as stiff (competent) soil. Ultimate bearing capacity values were found between 12.36 and 14 T/m², which reflect stiff consistency, especially from a depth 1 to 10 meter. However, it indicated that the soil site was capable of bearing light and medium weights. Based on these results, the cover layer is considered a soft filling material with a thickness of 1 m. The soil was divided into four layers; the first one is stiff to very stiff sand silty clay (2 to 3) m in depth, the second layer is medium to stiff at 3 to 6 m depth, the third layer is stiff (6 to 9) m depth, and the fourth layer is soft silty clay at 9 to 15m depth.

**Keywords:** Cross-Hole; Injection; Elasticity modulus; Bearing capacity; Geotechnical Parameters

## 1. Introduction

The technique of refraction survey through boreholes is very important in identifying the foundations of sites designated for the construction of facilities, dams, roads, etc. It can also be considered as one of the methods that gives an indication of the presence of weak zones and utilities in the foundations of the soils under study. For civil engineering, construction of basic structures frequently requires unique records of the soil properties and locations (Gupta, 2013), since the wave velocities can't be in confidence when measured on the earth surface, thus and in this case, seismic refraction survey in the drilled bore-holes was used in this research owing to its high-frequency source that may solve thin layer problem if exist. The coordinates of the drilled boreholes of 15 meters in depth, which were used

DOI: 10.46717/igj.57.1E.4ms-2024-5-15

in this research and the distances between the sources and receivers is illustrated in Table.1. This study presents the results of cross-borehole seismic testing at a selected site called “Al-Mawaddah Hospital Site” inside Basrah City, south of Iraq; where five boreholes were drilled in the site as shown in (Fig.1).

Khorshid et al. (2014) used seismic refraction technique in the site of the University of Tikrit, north of the central part of Iraq in order to evaluate the geotechnical properties of the underlying soil; depending on the compressional and shear waves velocities. Accordingly, Poisson's ratio, Material index and Plasticity index were calculated using the equations related to these velocities. Al-Khersan et al. (2012) used seismic refraction and electric methods to investigate the soil foundations underlying two sites in Hilla and Karbala cities (Middle part of Iraq) to construct Gas Power Plants; for each city.

**Table 1.** The coordinates of the drilled boreholes and distances between the sources and receivers in the study site

| Borehole No. | Coordination using UTM | | Distances between boreholes (sources and receivers) (m) | |
|---|---|---|---|---|
| | Easting | Northing | | |
| 1 | 47801038 | 30499677 | BH.4- BH.1 | 17 |
| 2 | 47801054 | 30499689 | BH.4- BH.2 | 13 |
| 3 | 47801067 | 30499695 | BH.4- BH.3 | 21 |
| 4 | 47801051 | 30499681 | BH.5- BH.2 | 11.8 |
| 5 | 47801064 | 30499685 | BH.5- BH.3 | 11.8 |

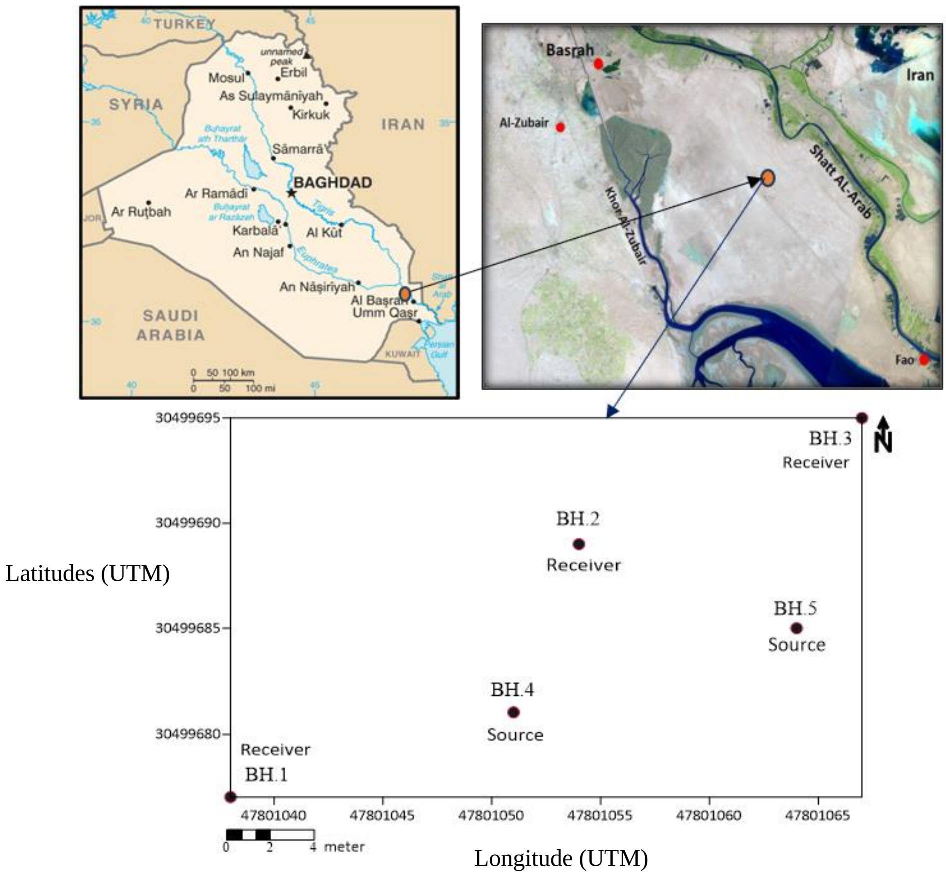


**Fig. 1**. Location of the study site shows the drilled boreholes (sources and receivers)

Khorshid et al. (2014) acquired the elastic modules and bearing capacity values from standard penetration test of the studied soils. They identified five subsurface layers, depths, thicknesses, and the resistivity values of these layers. These indicated that the subsurface layers of Karbala site have resistivity values better than Hilla because of the dry soil and high gypsum content of Karbala site. Al-Amar and Al-Khalidi (2023) studied the use of down-hole seismic technique in a site located south of Baghdad. A number of geotechnical properties such as Poisson's ratio, Lames constant, Compressibility modulus, Bulk modulus, Youngs modulus, Shear modulus, Material index, Concentration index and Coefficient of lateral pressure were determined using compressional and shear velocities. The results of the geotechnical assessment of the site confirmed weakness in the soil and this may lead to a difference in bearing capacity. Jedi and Al-Khalidi (2023) performed their geotechnical and cross-hole seismic investigations to locate the dynamic modulus of the sub-surface soil sections in Hilla City, Middle of Iraq. Saify and Alkhalidy (2023) also found that there is a wide difference in Poisson's ratio at depth 1 to 10 m., which indicates that the soil is sandy clay.

The main objective of this study is to calculate the elastic moduli and the geotechnical properties of the concerned site to divide the underlying strata and improve the weak soft zone of the studied soil between depth 1 and 15 m, and then to construct the required hospital.

## 2. Geology, Stratigraphy and Tectonic Settings

Geologically, the study area is characterized by the existence of the Quaternary sediments (Mesopotamian Basin) during Pleistocene-Recent (about 85 m thick). Erosion and deposition processes on the Dibddiba Formation, whether fluctuations and sea level action have influenced on the types and nature of the sediments during this period. Clay, silt, sand and igneous fragments were distributed among the area to form a wide flat area around the Basrah Governorate, which is consider as an economic importance used for quarrying purposes. The Mesopotamian Basin represented by the Quaternary sediments have thickness of about 120 m and is surrounded by Tertiary sediments. The source of these sediments is the mountains of Taurus and Zagros and the drainage of the Tigris, Euphrates and Shatt Al-Arab rivers. The Quaternary sediments are considered as important sources owing to their value in constructions and the existence of underground water aquifers. The Quaternary sediments are classified into two main groups; firstly, the cohesive sediments represented by the recent silty and Al-Hammar Formation sediments and secondly, the cohesionless sediments represented by sands of the Dibddiba Formation. According to the consistency of cohesive sediments and the compactness of cohesionless sediments, six strata can be identified starting from the surface to 15-meter depth as follows: 1) fill materials, 2) stiff to very stiff grayish sandy silty clayey soil, 3) soft gray silty clayey soil, 4) stiff brownish silty sandy clayey soil, 5) very stiff grayish silty sandy clayey soil 6) and very dense grayish silty sandy soil, as shown in Fig. (2) (Al-Siyab et al., 1982)

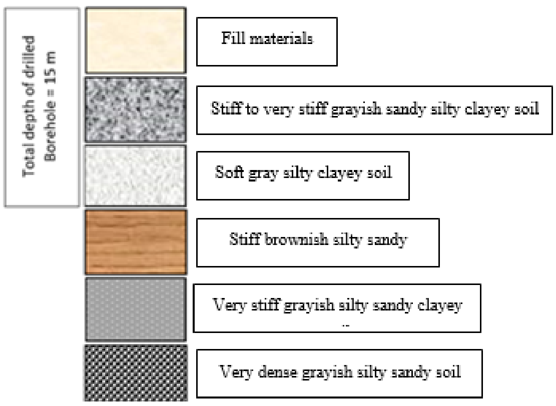


**Fig. 2.** Soil type column in the studied area

Tectonically, the study area is positioned in the Zubair-Subzone, south of the Mesopotamian Zone, representing the eastern side of the Stable part of the Arabian Shelf (Fig. 3). It is located within the Basrah block between the Takhadid-Qurna Transversal Fault at the north and Al-Batin as the southern boundary. The thick column of sediments was affected by the Alpine movement and subsurface anticlines with wide synclines (Buday and Jassim, 1987). As a result of tectonic activity, a number of subsurface geological structures appeared in the region, such as Al-Batin Fan, Jabal Sanam and the sand dunes located within the study area. The region was exposed to a neotectonics movements caused a fault may separate between Warba island and Khor Al-Zubair. These movements directly influenced the subsurface structures and thus the geomorphology of the region (Hussien et al., 1991).

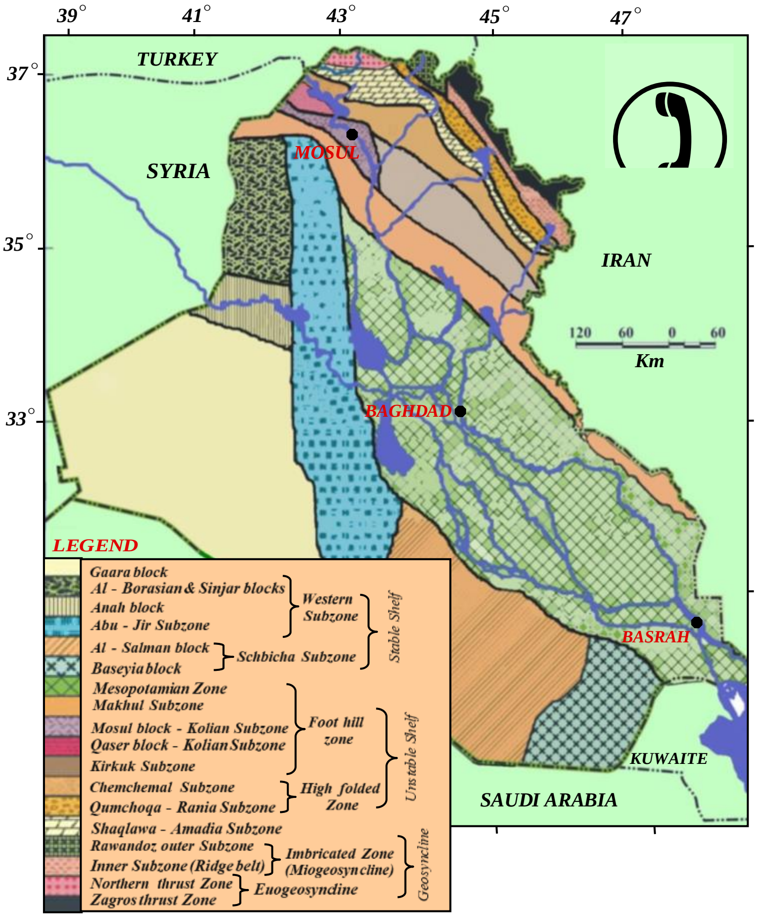


**Fig. 3.** Tectonic divisions of Iraq (Al-Khersan et al., 2007)

## 3. Seismicity and Earthquakes

In Iraq, the seismic magnitude of earthquakes is intermediate and the focal depth is shallow. Seismicity of the Stable Shelf was resulted from local deformation, but the seismicity of folded area is coming from the movements of the Arabian Plate towards the north and north east. According to the seismic zoning map (Fig. 4), the investigated sites lie within no damage zone (zone with green colour). The Stable Shelf (including the Mesopotamian Zone) shows weak seismic activity. There is a sharp boundary between the Folded (unstable) and unfolded (stable) Zones, which suggests that stresses resulting from the movement of the Arabian Plate towards the north and northeast are not transmitted to the unfolding region (Buday and Jassim, 1987).

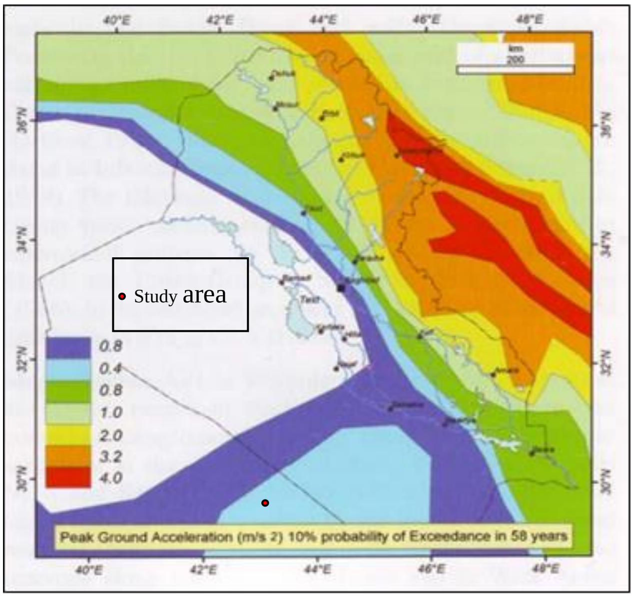


**Fig. 4**. Seismic zoning map derived from the global seismic hazard map (Jassim and Goff, 2006)

## 4. Methods and Materials

### 4.1. Injection Method

The ground enhancement or soil stabilization method that includes injection of a fluid-like material under managed stress using single or more than one channels into soil or rock strata to enhance their mechanical behavior. However, improved cement is added with quick-hardening materials. The drilling network of micro-piles using 105 verticals drilled next to each injection well to allow the exit of confined groundwater below the earth surface. Pipe of two meters long was used in casing the drilling wells and the operation was done according to the specification using ASTM. D4428/D44 (Park et al., 2008) (Fig. 5).

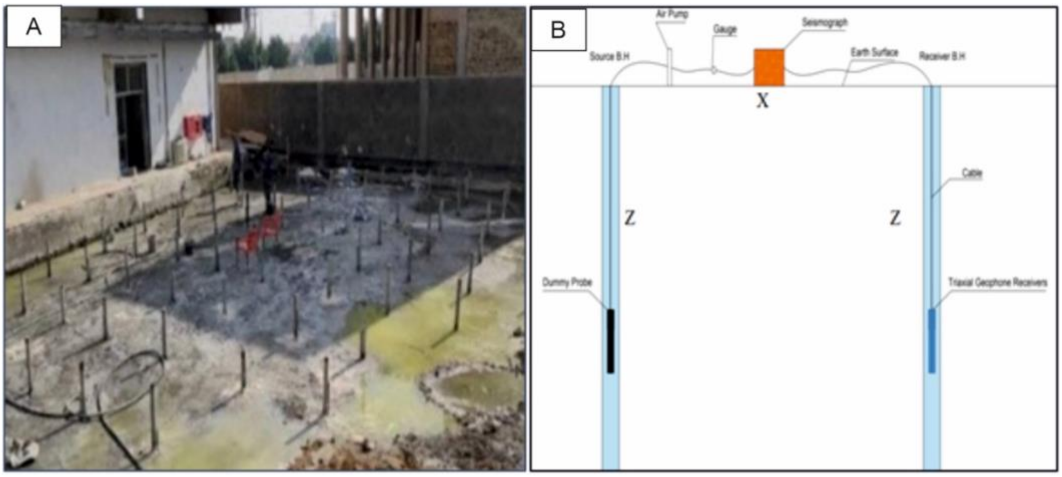


**Fig. 5**. A. The injection piles network in the study site, and B. sketch for Cross-hole survey configuration (Gupta, 2013)

### 4.2. Seismic Refraction Survey in Boreholes

Construction of foundation systems for civil structures often requires detailed information about the site soil properties (Gupta, 2013; Mohsain and Al-Khalidy, 2022). As subsurface wave velocities cannot be reliable on the surface, thus, seismic survey in boreholes can be used owed to their high-frequency sources that may solve thin layer and velocity inversion problems. There are three important survey techniques: cross-hole, cross borehole-hole and up-hole (Crice, 2002). Two types of body waves can be used for seismic shooting, which are P and S-waves. P-wave travels faster from S- wave and thus arrive first at the first geophone. S-wave has an important advantage that its propagation velocity is not influenced by groundwater content. However, due to the lower speed of Vs, it can be measured with greater accuracy as the arrival time interval is longer than in the case of P-wave (Massarsch, 2007).

The seismic refraction survey in boreholes was carried out at Al-Mawaddah Hospital Site using the three channels seismic refraction system (ABEM Pro Terraloc System and Cross-Borehole Instrument, ABEM AB, made in Sweden). The survey was conducted on 30th January, 2021. Cross-borehole seismic survey is the simplest and cheapest method in the suite of borehole seismic technique, as they require only a single borehole. Seismic energy is generated on the surface at a fixed distance from the top of the borehole.

Cross-hole seismic technique was applied in the investigated site; for both P and S-wave velocity measurements individually. Eleven successive shot points were applied, which resulted in three records for S-wave and one for P-wave per each borehole. The records were obtained using an array of three geophones. Two geophones for S-wave measurements and one for P-wave were used in this survey. The survey included one seismic test between boreholes 1 and 2 and boreholes 3, 4 and 5, where one borehole was chosen to represent the source and the other boreholes are the receivers. The offset between boreholes is 2 m. The survey started from 15.0 m depth up towards earth surface and the interval between traces is 1.0 m.

## 5. Result and Discussion

### 5.1. Picking of First Arrival Times and Velocity Calculation

The first arrival times for all seismograms (seismic sections) between boreholes were picked using program SeisTW. Travel time of compressional ($T_p$) and shear ($T_s$) waves including ($T_{sh}$, $T_{sv}$) were recorded by the horizontal waves travelling between borehole source and receiver indeed as shown in (Fig.6).

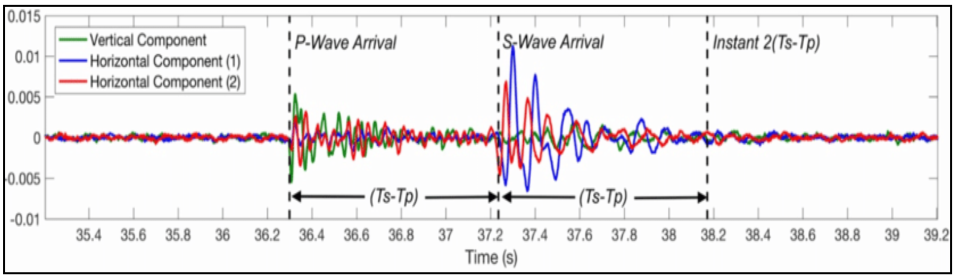


**Fig. 6**. Seismogram between BH.1 and BH.4 showing ($T_p$, $T_{sv}$ and $T_{sh}$)

Compressional ($V_p$) and shear ($V_s$) wave velocities can be determined from the travel time between the source and one or more receivers (X) for each depth interval sequentially (Stokoe and Santamarina, 2000). The $V_p$ and Vs were obtained using the equations (1, and 2) as illustrated in (Table.2). However, the time will change owing to the horizontal variations in types and densities of the layers between boreholes, as well as the conditions of the recorded profile.

$$V_p = X/T_p \tag{1}$$

$$V_s = X/T_s \tag{2}$$

There is a direct correlation between seismic velocity and the density of the subsurface materials. The bulk density-ρ can be given as follows (Uyanik, 2010):

$$\rho = 16 + 0.002\ V_p \tag{3}$$

**Table 2.** First arrival times for all seismic sections between boreholes

| Depth (m) | First arrival times for all seismic sections between boreholes | | | | | | | | | |
|---|---|---|---|---|---|---|---|---|---|---|
| | (BH.4-BH.1) = 17 m | | (BH.4-BH.2) = 13 m | | (BH.4-BH.3) = 21 m | | (BH.5-BH.2) = 11.8 m | | (BH.5-BH.3) = 11.8 m | |
| | $T_p$ | $T_s$ | $T_p$ | $T_s$ | $T_p$ | $T_s$ | $T_p$ | $T_s$ | $T_p$ | $T_s$ |
| 1 | 13.9 | 23.22 | 10.4 | 18.54 | 14.93 | 16.92 | 9.48 | 14.93 | 9.72 | 15.94 |
| 2 | 13.93 | 23.6 | 10.44 | 18 | 15.92 | 16.93 | 9.47 | 15.92 | 9.75 | 15.92 |
| 3 | 14 | 22.6 | 10.51 | 16.45 | 16.09 | 16.85 | 9.67 | 16.09 | 9.82 | 16.61 |
| 4 | 14.01 | 23.34 | 10.75 | 18.28 | 15.08 | 17.07 | 9.74 | 15.08 | 9.9 | 16.36 |
| 5 | 14.08 | 22.04 | 10.73 | 18 | 16.12 | 17.35 | 9.74 | 16.12 | 9.9 | 15.92 |
| 6 | 13.94 | 23.84 | 10.83 | 16.86 | 16.36 | 17.21 | 9.61 | 16.36 | 9.61 | 14.93 |
| 7 | 14.08 | 24.42 | 10.83 | 18.03 | 14.91 | 17.28 | 9.68 | 14.91 | 9.81 | 16.07 |
| 8 | 4.26 | 22.35 | 10.9 | 18.17 | 16.57 | 17.4 | 9.81 | 16.57 | 9.74 | 14.82 |
| 9 | 14.43 | 23.9 | 11.13 | 18.54 | 16.83 | 17.32 | 9.81 | 16.83 | 9.9 | 16.34 |
| 10 | 14.55 | 23.21 | 11.13 | 18.75 | 16.43 | 17.84 | 9.9 | 16.43 | 9.96 | 16.76 |
| 11 | 14.55 | 23.02 | 11.2 | 18.62 | 16.09 | 17.91 | 10.04 | 16.09 | 9.74 | 16.05 |
| 12 | 14.65 | 23.57 | 11.2 | 18.03 | 17.02 | 17.91 | 10 | 17.02 | 9.81 | 16.59 |
| 13 | 14.56 | 24.25 | 11.18 | 19.03 | 17.39 | 17.84 | 10.03 | 17.39 | 9.81 | 17.07 |
| 14 | 14.68 | 24.69 | 11.2 | 18.43 | 18.32 | 17.98 | 10.02 | 18.32 | 9.81 | 18.96 |
| 15 | 14.73 | 24.45 | 11.22 | 18.36 | 16.83 | 18.2 | 10 | 16.83 | 9.9 | 18.34 |

The results of depths, $V_p$ and $V_s$ waves for cross-hole seismic survey and the densities are illustrated in the Table (3). Table (3) shows that the average of $V_p$ ranges from 1234.4 m/sec to 1168.8 m/sec starting from 1.0 to 15.0 m depths, respectively. The average of $V_s$ ranges between 756 m/sec and 691.8 m/sec from 1.0 to 15.0 m, respectively. The important relationships between average velocities (x-axis) versus depths (y-axis) for both P and S waves were plotted for this type of survey (Fig. 7). It is noted from this figure and through changes in the values of $V_p$ and $V_s$ with depth that three layers can be distinguished within the soil of the study site, these are: the first layer from the depth of 2-3 m, the second layer from the depth of 4-8 m and the third layer from the depth of 9-15 m.

Generally, it seems that the values of $V_p$ and $V_s$ waves are slight, with an insignificant decrease with depth. It gives the variations in lithology of soil and its components (Al-Amar and Al-Khalidi, 2018). The soil does not have sufficient rigidity, where the velocity is affected by the density and water content of the soil (Al-Amar et al., 2018).

**Table 3**. $V_p$, $V_s$ waves and densities of the selected cross-borehole profiles

| Depth (m) | Distance between the sources (BH 4 and 5) and the receivers (BH 1, 2 and 3) | | | | | | | | | | | | | | | Average velocities (m/sec) | | Average density (gm/cm^3) |
|---|---|---|---|---|---|---|---|---|---|---|---|---|---|---|---|---|---|---|
| | (BH.4-BH.1) = 17 m | | Density (gm/cm^3) | (BH.4-BH.2) = 13 m | | Density (gm/cm^3) | (BH.4-BH.3) = 21 m | | Density (gm/cm^3) | (BH.5-BH.2) = 11.8 m | | Density (gm/cm^3) | (BH.5-BH.3) = 11.8 | | Density (gm/cm^3) | | | |
| | $V_p$ | $V_s$ | | $V_p$ | $V_s$ | | $V_p$ | $V_s$ | | $V_p$ | $V_s$ | | $V_p$ | $V_s$ | | $V_p$ | $V_s$ | |
| 1 | 1223 | 732 | 0.184 | 1250 | 701 | 0.185 | 1244 | 790 | 0.185 | 1244 | 790 | 0.185 | 1214 | 740 | 0.184 | 1234.4 | 756 | 0.185 |
| 2 | 1220 | 720 | 0.184 | 1245 | 722 | 0.185 | 1245 | 741 | 0.185 | 1245 | 741 | 0.185 | 1210 | 741 | 0.184 | 1232 | 751 | 0.185 |
| 3 | 1214 | 752 | 0.184 | 1237 | 790 | 0.185 | 1220 | 733 | 0.184 | 1220 | 733 | 0.184 | 1201 | 710 | 0.184 | 1223.6 | 753.2 | 0.184 |
| 4 | 1213 | 728 | 0.184 | 1209 | 711 | 0.184 | 1211 | 782 | 0.184 | 1211 | 782 | 0.184 | 1192 | 721 | 0.184 | 1207.2 | 741.8 | 0.184 |
| 5 | 1207 | 771 | 0.184 | 1211 | 722 | 0.184 | 1211 | 732 | 0.184 | 1211 | 732 | 0.184 | 1192 | 746 | 0.184 | 1206.2 | 752.2 | 0.184 |
| 6 | 1219 | 713 | 0.184 | 1200 | 771 | 0.184 | 1228 | 721 | 0.185 | 1228 | 721 | 0.185 | 1228 | 790 | 0.185 | 1219.2 | 751.6 | 0.184 |
| 7 | 1207 | 696 | 0.184 | 1200 | 721 | 0.184 | 1219 | 791 | 0.184 | 1219 | 791 | 0.184 | 1202 | 734 | 0.184 | 1208.6 | 738.4 | 0.184 |
| 8 | 1192 | 760 | 0.184 | 1192 | 715 | 0.184 | 1202 | 712 | 0.184 | 1202 | 712 | 0.184 | 1211 | 796 | 0.184 | 1200.8 | 747.6 | 0.184 |
| 9 | 1178 | 711 | 0.184 | 1168 | 701 | 0.183 | 1202 | 701 | 0.184 | 1202 | 701 | 0.184 | 1192 | 722 | 0.184 | 1190.4 | 723.4 | 0.184 |
| 10 | 1168 | 732 | 0.183 | 1168 | 693 | 0.183 | 1192 | 718 | 0.184 | 1192 | 718 | 0.184 | 1184 | 704 | 0.184 | 1177.8 | 718.2 | 0.184 |
| 11 | 1168 | 738 | 0.183 | 1160 | 698 | 0.183 | 1175 | 733 | 0.184 | 1175 | 733 | 0.184 | 1211 | 735 | 0.184 | 1177.2 | 726.8 | 0.184 |
| 12 | 1160 | 721 | 0.183 | 1160 | 721 | 0.183 | 1211 | 693 | 0.184 | 1211 | 693 | 0.184 | 1202 | 711 | 0.184 | 1181 | 721.4 | 0.184 |
| 13 | 1167 | 701 | 0.183 | 1162 | 683 | 0.183 | 1202 | 678 | 0.184 | 1202 | 678 | 0.184 | 1202 | 691 | 0.184 | 1182 | 697.2 | 0.184 |
| 14 | 1158 | 688 | 0.183 | 1160 | 705 | 0.183 | 1202 | 644 | 0.184 | 1202 | 644 | 0.184 | 1202 | 622 | 0.184 | 1178 | 674 | 0.184 |
| 15 | 1154 | 695 | 0.183 | 1160 | 708 | 0.183 | 1184 | 701 | 0.184 | 1184 | 701 | 0.184 | 1192 | 643 | 0.184 | 1168.8 | 691.8 | 0.184 |

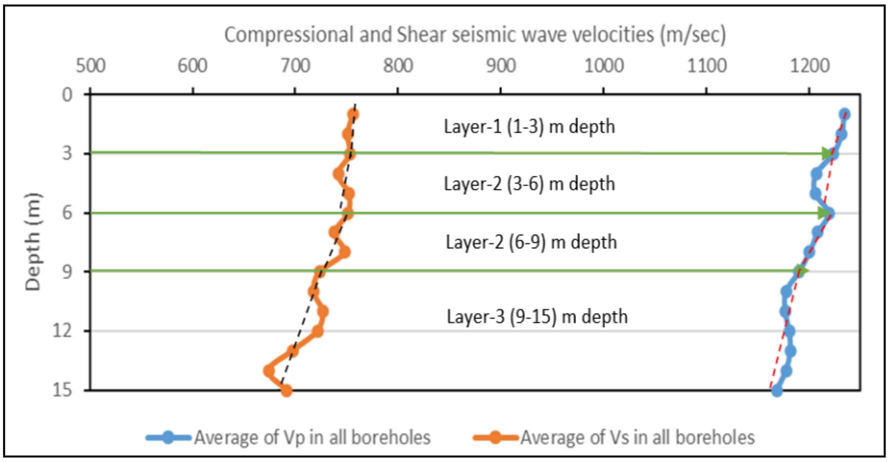


**Fig. 7.** The relation between average velocities of $V_p$, $V_s$ and depths for all selected boreholes in the study area

### 5.2. Calculation of the Elastic Modulus from Seismic Cross-Hole Data

Calculation of the elastic modulus and its geotechnical properties of the studied site provide a solution to many construction problems due to the large extent of soil damage; particularly against earthquakes, sea waves, machine vibrations, nuclear explosions, etc. They were; therefore, considered part of the geotechnical properties of soils (Swain, 1962). The important factors that impact the dynamic properties of soil are void ratio, overburden pressure and saturation percentage. The most significant of these transactions are Poisson's Ratio-σ, Shear-μ, Young (E) and Bulk (K) modulus. The amounts of changes in elastic modulus for each 1.0 m subsurface soil intervals at the site between the sources and the receivers (BH.4 towards BH 1, 2, and 3 and BH.5 towards BH 2 and 3) were calculated using the equations below; as shown in (Table.4) (Al-Sinawi et al., 1990).

$$\text{Poisson's Ratio } (\sigma) = [(V_p/V_s)^2 - 2]/[2\,(V_p/V_s)^2 - 2] \tag{4}$$

$$\text{Dynamic Shear Modulus } (\mu) = (V_s)^2 \rho \tag{5}$$

$$\text{Young's Modulus } (E) = 2\,\mu\,(1+\sigma) \tag{6}$$

$$\text{Bulk Modulus } (K) = E\,/\,3\,(1-2\,\sigma) \tag{7}$$

Table 5 shows the substantial values of Poisson's ratio and Young's modulus according to different characters of materials, while the value of shear modulus is zero in the liquid and gaseous mediums. The average elastic moduli had been calculated using seismic waves' velocities for both $V_p$ and $V_s$ related to all boreholes (Table 6).

The relationship between width strain and length strain; while the body is under compressional and tensile stress is called "Poisson's Ratio". It has been showed from Table (3) that the average value of Poisson's ratio ranges between 0.1471597 and 0.309449 in BH. 4; from depths 1.0 to 15.0 m, respectively. This is due to the lithological variations, difference in ratio consolidation, moisture and percentage of water content in the soil which are regular with engineering properties output. The difference of σ suggests that the soil in these layers is classified according to Table (5) within unsaturated clayey soil (medium) to sandy clayey soil (stiff) in the investigated area. The deformation by means of shearing force is called "Shear Modulus", which is directly proportional with the shear wave's velocity. The Shear modulus reflects the geotechnical properties, which increase with cohesion and stiffness of soil (Ameen, 2006). The minimum and maximum values of this moduli are 84586 MPa and 106085 MPa, respectively.

**Table 4.** Values of the Elastic modulus for all studied boreholes

| Depth (m) | Between (BH.4-BH.1) | | | | Between (BH.4-BH.2) | | | | Between (BH.4-BH.3) | | | |
|---|---|---|---|---|---|---|---|---|---|---|---|---|
| | σ | μ (MPa) | E (MPa) | K (MPa) | Σ | μ (MPa) | E (MPa) | K (MPa) | σ | μ (MPa) | E (MPa) | K (MPa) |
| 1 | 0.220897 | 98838 | 241342 | 144.12 | 0.270609 | 231020 | 63.44096 | 142.28 | 0.204382 | 115384 | 277932 | 226.64 |
| 2 | 0.232784 | 95593 | 235691 | 147.00 | 0.24664 | 240316 | 69.51049 | 162.39 | 0.199962 | 101525 | 243652 | 203.08 |
| 3 | 0.188699 | 104211 | 247751 | 132.64 | 0.1556 | 266473 | 93.27722 | 285.42 | 0.231376 | 99076 | 244000 | 175.76 |
| 4 | 0.218508 | 97655 | 237986 | 140.91 | 0.23565 | 230095 | 68.39187 | 162.74 | 0.211527 | 112655 | 272969 | 215.08 |
| 5 | 0.15536 | 109460 | 252932 | 122.32 | 0.224258 | 235133 | 71.57564 | 174.75 | 0.178072 | 98709 | 232574 | 217.68 |
| 6 | 0.239989 | 93733 | 232456 | 149.00 | 0.148492 | 251238 | 89.59228 | 281.99 | 0.146956 | 95942 | 220082 | 249.60 |
| 7 | 0.250926 | 89200 | 223166 | 149.33 | 0.217527 | 232915 | 71.99684 | 178.46 | 0.202689 | 115363 | 277492 | 228.18 |
| 8 | 0.157521 | 106186 | 245825 | 119.63 | 0.218996 | 229131 | 65.08084 | 174.38 | 0.119635 | 93298 | 208919 | 291.05 |
| 9 | 0.213476 | 92793 | 225205 | 131.00 | 0.218499 | 219582 | 62.59695 | 167.49 | 0.210263 | 90437 | 218906 | 173.52 |
| 10 | 0.176591 | 98249 | 231197 | 119.15 | 0.228358 | 216335 | 60.40457 | 157.89 | 0.226554 | 94774 | 232491 | 171.03 |
| 11 | 0.16773 | 99866 | 233233 | 116.99 | 0.216213 | 217108 | 62.24389 | 167.36 | 0.208395 | 98593 | 238277 | 190.57 |
| 12 | 0.185234 | 95235 | 225751 | 119.53 | 0.185234 | 225751 | 69.03841 | 203.12 | 0.230901 | 88471 | 217799 | 157.21 |
| 13 | 0.217744 | 90093 | 219422 | 129.56 | 0.236076 | 211318 | 58.08706 | 149.19 | 0.253195 | 84600 | 212041 | 139.58 |
| 14 | 0.227217 | 86698 | 212794 | 130.01 | 0.207141 | 219832 | 64.2335 | 176.88 | 0.317149 | 76328 | 201071 | 105.67 |
| 15 | 0.215429 | 88432 | 214966 | 125.90 | 0.201522 | 220675 | 65.24047 | 182.51 | 0.294797 | 90261 | 233738 | 132.15 |

Continued Table.4

| **Depth (m)** | **Between (BH.5-BH.2)** | | | | **Between (BH.5-BH.3)** | | | |
|---|---|---|---|---|---|---|---|---|
| | **Σ** | **μ (MPa)** | **E (MPa)** | **K (MPa)** | **Σ** | **μ (MPa)** | **E (MPa)** | **K (MPa)** |
| 1 | 0.162077 | 115384 | 268169 | 275.76 | 0.204382 | 101131 | 243600 | 198.65 |
| 2 | 0.226399 | 101525 | 249021 | 183.32 | 0.199962 | 101383 | 243312 | 202.80 |
| 3 | 0.217547 | 99076 | 241260 | 184.83 | 0.231376 | 92927 | 228855 | 164.85 |
| 4 | 0.142382 | 112655 | 257390 | 301.29 | 0.211527 | 95716 | 231924 | 182.74 |
| 5 | 0.212138 | 98709 | 239299 | 188.01 | 0.178072 | 102461 | 241413 | 225.95 |
| 6 | 0.236961 | 95942 | 237353 | 166.94 | 0.146956 | 115107 | 264045 | 299.46 |
| 7 | 0.13635 | 115363 | 262186 | 320.48 | 0.202689 | 99234 | 238696 | 196.27 |
| 8 | 0.229734 | 93298 | 229463 | 166.47 | 0.119635 | 116597 | 261092 | 363.73 |
| 9 | 0.242291 | 90437 | 224699 | 154.57 | 0.210263 | 95810 | 231911 | 183.83 |
| 10 | 0.215287 | 94774 | 230355 | 178.33 | 0.226554 | 91015 | 223269 | 164.25 |
| 11 | 0.18145 | 98593 | 232964 | 213.98 | 0.208395 | 99189 | 239719 | 191.72 |
| 12 | 0.236749 | 88471 | 218834 | 154.05 | 0.230901 | 92932 | 228781 | 165.14 |
| 13 | 0.251063 | 84600 | 211680 | 140.52 | 0.253195 | 87756 | 219951 | 144.78 |
| 14 | 0.286349 | 76328 | 196369 | 114.29 | 0.317149 | 71091 | 187275 | 98.42 |
| 15 | 0.227302 | 90261 | 221554 | 162.45 | 0.294797 | 75884 | 196510 | 111.10 |

**Table 5**. Typical Poisson's ratio and young's modulus for different soils

| Poisson's ratio (σ) (modified from Hunt, 1986) | | | Young's modulus (Mpa) (modified from Dobrin, 1976) | | |
|---|---|---|---|---|---|
| **Soil Type** | **Description** | **Values** | **Soil Type** | **Description** | **Values** |
| Clay | Saturated clay soil (soft) | 0.4-0.5 | Clay | Very soft clay | 5-50 |
| | Unsaturated clay soil (medium) | 0.1-0.3 | | Soft clay | 50-200 |
| | Sandy clay soil (stiff) | 0.2-0.3 | | Medium clay | 200-500 |
| Sand | Silty soil (loose-medium) | 0.3-0.35 | | Stiff clay, silty clay | 500-1000 |
| | Concrete (dense) | 0.15 | | Clay shale | 250-2000 |
| | | | Sand | Loose sand | 100-250 |
| | | | | Dense sand | 250-1000 |
| | | | | Dense sand and gravel | 1000-2000 |
| | | | | Silty sand | 250-2000 |
| | | | | Very soft clay | 5-50 |

**Table 6**. The average values of Poisson's ratio, Shear, Young, and Bulk modulus for BH 4 and BH 5

| Depth (m) | Averages for BH 4 | | | | Averages for BH 5 | | | |
|---|---|---|---|---|---|---|---|---|
| | Σ | μ (MPa) | E (MPa) | K (MPa) | σ | μ (MPa) | E (MPa) | K (MPa) |
| 1 | 0.1938057 | 101459 | 242245 | 171.02 | 0.1832295 | 108021 | 255627 | 237.21 |
| 2 | 0.2065712 | 97816 | 236044 | 170.83 | 0.2131805 | 101333 | 245870 | 193.06 |
| 3 | 0.2279187 | 106085 | 260527 | 197.94 | 0.2244615 | 95893 | 234834 | 174.84 |
| 4 | 0.1942407 | 100970 | 241164 | 172.91 | 0.1769545 | 103931 | 244645 | 242.01 |
| 5 | 0.1865885 | 101319 | 240448 | 171.58 | 0.195105 | 100503 | 240222 | 206.98 |
| 6 | 0.1694572 | 99571 | 232887 | 226.86 | 0.1919585 | 105343 | 251129 | 233.20 |
| 7 | 0.1861042 | 99766 | 236666 | 185.32 | 0.1695195 | 107101 | 250513 | 258.38 |
| 8 | 0.1471597 | 97736 | 224237 | 195.02 | 0.1746845 | 104681 | 245934 | 265.10 |
| 9 | 0.21827 | 91108 | 221988 | 157.34 | 0.226277 | 93116 | 228373 | 169.20 |
| 10 | 0.2237372 | 93645 | 229194 | 149.36 | 0.2209205 | 92895 | 226834 | 171.29 |
| 11 | 0.2016587 | 95844 | 230344 | 158.30 | 0.1949225 | 99056 | 236728 | 202.85 |
| 12 | 0.232363 | 92957 | 229115 | 159.96 | 0.233825 | 90740 | 223915 | 159.60 |
| 13 | 0.252662 | 86709 | 6409.26 | 139.44 | 0.252129 | 86230 | 5961.619 | 142.65 |
| 14 | 0.309449 | 84586 | 6310.404 | 137.52 | 0.301749 | 73743 | 6000.241 | 106.36 |
| 15 | 0.2779232 | 90169 | 6457.427 | 146.85 | 0.2610495 | 82983 | 6120.85 | 136.78 |

The ratio of the longitudinal stress to strain is called "Young's Modulus". The solid materials have high Young's modulus values, while low values represent material with less hardness. The results range between 5961.619 MPa in BH 5 to 260527 MPa in BH 4. A change in size without the shape represents the ratio between compressive stress and volume change is called "Bulk Modulus" (Dobrin, 1976). Its values range between 106.36 MPa in BH 5 to 226.86 MPa in BH 4, which indicate compacted layers underlying the ground surface. The cement grouting material with plasticizing and hardening chemical additives was added to the soil, which could lead to the non-conformity of the Shear and Young's modulus values with the typical values of the calculated values for natural soils as mentioned in Table 6. It indicates that the soil after injection may behave bearable when subjected to great stresses.

The relationships between the elastic modulus versus depth is plotted in Fig. 8. Similar behavior of Poisson's ratio, shear and young's modulus can be seen perfectly in these plots, while there is a great difference in the behavior of Bulk modulus.

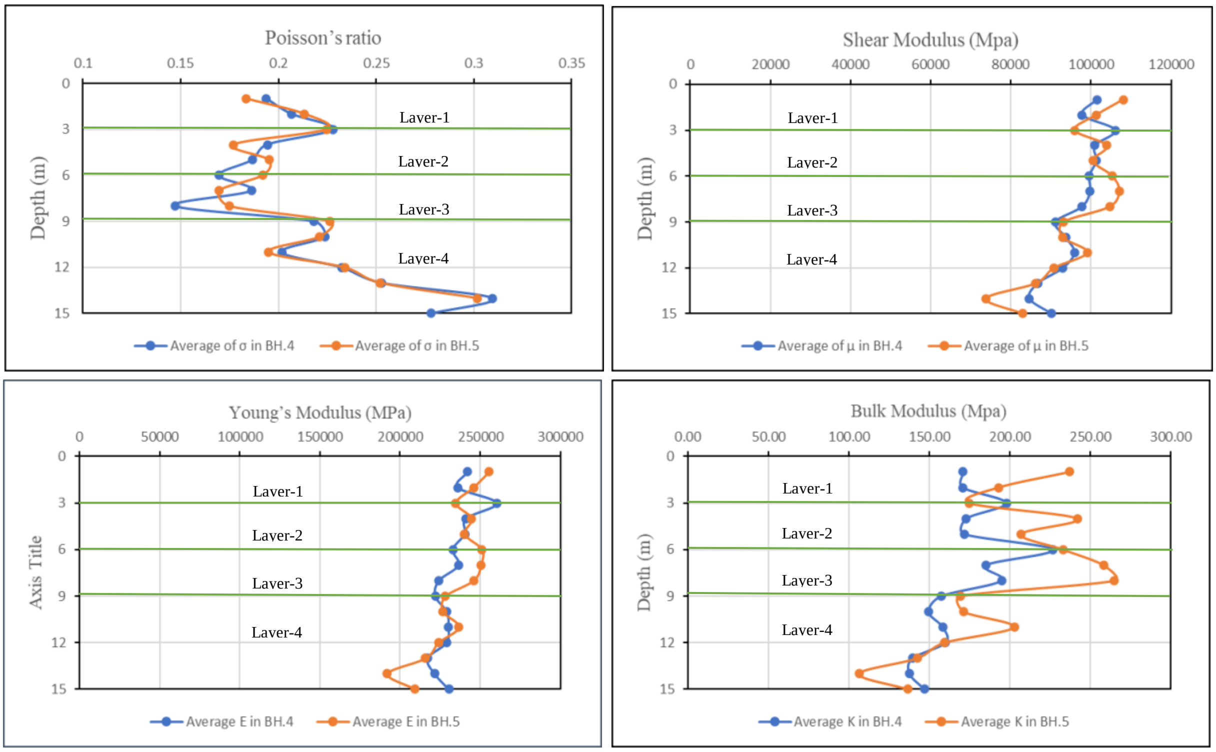


**Fig. 8.** Behavior of the average values of Poisson's ratio, shear, young, and bulk modulus of BH. 4 and BH. 5; with depth

### 5.3. Geotechnical Properties

To assess the suitability of the subsurface conditions for engineering buildings, the geotechnical parameters of shallow soil were computed from the values of $V_p$ and $V_s$. Poisson's ratio, Young's modulus, Shear modulus, and Bulk modulus were acquired. Then, Material Index-Im, Concentration Index-Ic, Coefficient of Lateral Earth Pressure at Rest-Ko, and Effective angle of internal friction (Ø) were determined.

The Ultimate Bearing Capacity-Qult before and after injection (treatment) was also calculated depending on $V_p$, $V_s$, and Standard Penetration Test (SPT) as illustrated in Table 7. The behaviors of the average values of the studied geotechnical properties of BH.4 and BH.5 with depth are constructed individually as shown in Fig. 9.

#### *5.3.1. Material Index (Im)*

This is the most important geotechnical property because it represents the degree of materials efficiency. It depends on many elastic moduli and wave velocities, where it is derived according to equation (8).

$$I_m = [3 (V_s/V_p)^2 - 1] / [1 - (V_s/V_p)^2] \quad (8)$$

The limits of the Material Index lie between -1; when μ = 0 for liquid material and 1 (Yilmaz et al., 2006). The competence of soil as foundation materials can be classified according to the values of Poisson's ratio and material index as illustrated in Table 8. The results indicate that the soil of the study site is fairly to moderately competent soil material because the clay is mixed with silt and sand. Therefore, the values of the Material Index are lower than 0.5 in the study site.

**Table 7.** The average values of $I_m$, $I_c$, $K_o$ and Ø in BH 4 and BH 5 and Qult of soil

| Depth (m) | Average ($I_m$) | | Average ($I_c$) | | Average ($K_o$) | | Average (Ø) | | SPT in BH.4 before injection | Ultimate bearing capacity ($Q_{ult}$) in ($T/m^2$) | |
|---|---|---|---|---|---|---|---|---|---|---|---|
| | BH.4 | BH.5 | BH.4 | BH.5 | BH.4 | BH.5 | BH.4 | BH.5 | | before injection | after injection |
| 1 | 0.1285 | 0.26708 | 2.168 | 2.266 | 1.724 | 1.767 | 46.15 | 48.29 | 16 | 14 | 14 |
| 2 | 0.0598 | 0.14863 | 2.208 | 2.158 | 1.751 | 1.654 | 43.83 | 48.29 | 14 | 14 | 14 |
| 3 | 0.2508 | 0.10215 | 2.313 | 2.127 | 1.821 | 1.525 | 50.32 | 46.8 | 5 | 5 | 13.86 |
| 4 | 0.2046 | 0.29218 | 2.160 | 2.289 | 1.602 | 1.63 | 48.77 | 48.02 | 5 | 6 | 13.41 |
| 5 | 0.2109 | 0.21957 | 2.321 | 2.217 | 1.693 | 1.576 | 48.97 | 51.30 | 4 | 6 | 13.3 |
| 6 | 0.1660 | 0.23216 | 2.231 | 2.218 | 1.651 | 1.721 | 47.46 | 52.66 | 4 | 2 | 13.67 |
| 7 | 0.1935 | 0.32192 | 2.136 | 2.326 | 1.521 | 1.703 | 48.41 | 48.24 | 4 | 2 | 13.35 |
| 8 | 0.1916 | 0.30126 | 2.211 | 2.285 | 1.548 | 1.655 | 48.32 | 55.30 | 3 | 2 | 13.2 |
| 9 | 0.1009 | 0.09489 | 2.287 | 2.151 | 1.546 | 1.45 | 45.23 | 47.39 | 2 | 2 | 12.92 |
| 10 | 0.1730 | 0.11631 | 2.208 | 2.136 | 1.415 | 1.426 | 47.67 | 46.51 | 2 | 2.5 | 12.61 |
| 11 | 0.2461 | 0.22030 | 2.241 | 2.218 | 1.419 | 1.533 | 50.15 | 48.55 | 2 | 2.65 | 12.61 |
| 12 | 0.1639 | 0.02513 | 2.335 | 2.182 | 1.461 | 1.434 | 47.35 | 46.33 | 2 | 2.75 | 12.7 |
| 13 | 0.0393 | -0.03976 | 2.159 | 2.15 | 1.36 | 1.353 | 43.13 | 42.72 | 3 | 2.78 | 12.73 |
| 14 | 0.0226 | -0.23166 | 2.158 | 2.106 | 1.328 | 1.157 | 42.51 | 36.63 | 3 | 2.9 | 12.61 |
| 15 | 0.1350 | -0.04986 | 2.188 | 2.137 | 1.328 | 1.274 | 46.38 | 40.02 | 3 | 2.68 | 12.36 |

**Table 8**. Classification of soil's competency according to Poisson's ratio and Material Index

| Soil description | Incompetent to slightly competent | Fairly to moderately competent | Competent material | Very high competent material |
|---|---|---|---|---|
| Poisson's Ratio | 0.41- 0.49 | 0.35- 0.27 | 0.25- 0.16 | 0.12- 0.03 |
| Material Index (Im) | (-0.5) - (-1) | (-0.5) - 0.0) | (0.0) – 0.5) | > 0.5 |

It is noted from Table 7 that the average values of the Material Index in the study site ranges between -0.231 to 0.321, which indicates the existence of fairly to moderately competent soil according to the mentioned classification.

*5.3.2. Concentration Index (Ic)*

The concentration index is defined as a combination of material properties for soil or rock. It is considered a competence degree for the foundation and other civil engineering targets. It can be calculated through relation with Poisson's ratio or the relationship between Vp and Vs values as mentioned in equations 9 and 10 (Bowles, 1984; Al-Khfaji, 2004):

$$I_C = (1+\sigma) / \sigma \tag{9}$$

$$I_C = [3-4\,(V_s/V_p)] / [1-2(V_s/V_p)^2] \tag{10}$$

From Table 5, the average concentration index ranges from 2.136 to 2.241 in BH 4 and BH 5, respectively at the studied site, and this indicates that the soil after injection has become more efficient. The natural values of the soil in the study site refer to the normal density, stiffness, and natural cohesion of soil at shallow and deep depths.

### 5.3.3. Coefficient of Lateral Earth Pressure at Rest (Ko)

The coefficient of Lateral Earth Pressure at Rest is defined as the ratio between the horizontal effective stresses to the vertical effective stress (Menard, 2018). It is used to determine the soil stiffness and cohesion; as illustrated in Table (9).

**Table 9**. Coefficient's range of Lateral Earth Pressure at Rest (Craig, 2004)

| Type of soils | Coefficient of Lateral Earth Pressure at Rest ($K_o$) |
|---|---|
| Dense sand | 0.35 |
| Loose sand | 0.6 |
| Normally consolidated clays (Norway) | 0.5- 0.6 |
| Clay, OCR = 3.5 (London) | 1.0 |
| Clay, OCR = 20 (London) | 2.8 |

The coefficient of Lateral Earth Pressure at Rest parameter is derived from Poisson's ratio (equation 11) (Hunt, 1986) and (Vs/Vp) ratio (equation 12) (Craig, 2004).

$$K_o = \sigma / 1 - \sigma \tag{11}$$

$$K_O = 1 - 2\,[V_S/V_P]^2 \tag{12}$$

It seems that the tabulated values of Ko (Table 7) range from 1.274 to 1.821 in BH 5 and BH 4, respectively. Thus, the soil in the site is categorized as over-normally consolidated clay.

### 5.3.4. Effective angle of internal friction (∅)

This parameter evaluates the ability of a unit of rock or soil to hold up a shear stress. The friction angle (∅) can be calculated by using P-wave and S-wave velocity through equation 13 (Al-Khafaji, 2010)

$$\sin \emptyset = 2\,(V_s/V_p)^2 \tag{13}$$

Many factors affect the angle of friction such as water content, shape of grain, and mineral composition. Decreasing water content causes increasing density, which leads to an increase in the friction angle. Table (9) presents a typical range of true values of internal friction angle (∅) from several soil types (Bowles, 1988). The resulting values of this property range between 36.63 and 55.30, which correspond to dense gravely sandy soil (moderate competent).

**Table. 9.** Typical range of Internal friction values for several soil types

| Soil type | (Ø°) | | Soil type | (Ø°) | |
|---|---|---|---|---|---|
| | **Loose** | **Dense** | | **Loose** | **Dense** |
| Gravel | 32-36 | 35-50 | Fine sand | 27-33 | 33-39 |
| Coarse sand | 32-38 | 35-48 | Sandy gravel | 30-38 | 36-45 |
| Clayey sand | 28-32 | 35-40 | Gravely sand | 30-38 | 36-50 |
| Silty sand | 28-32 | 32-38 | Silt | 20-3 | 25-32 |

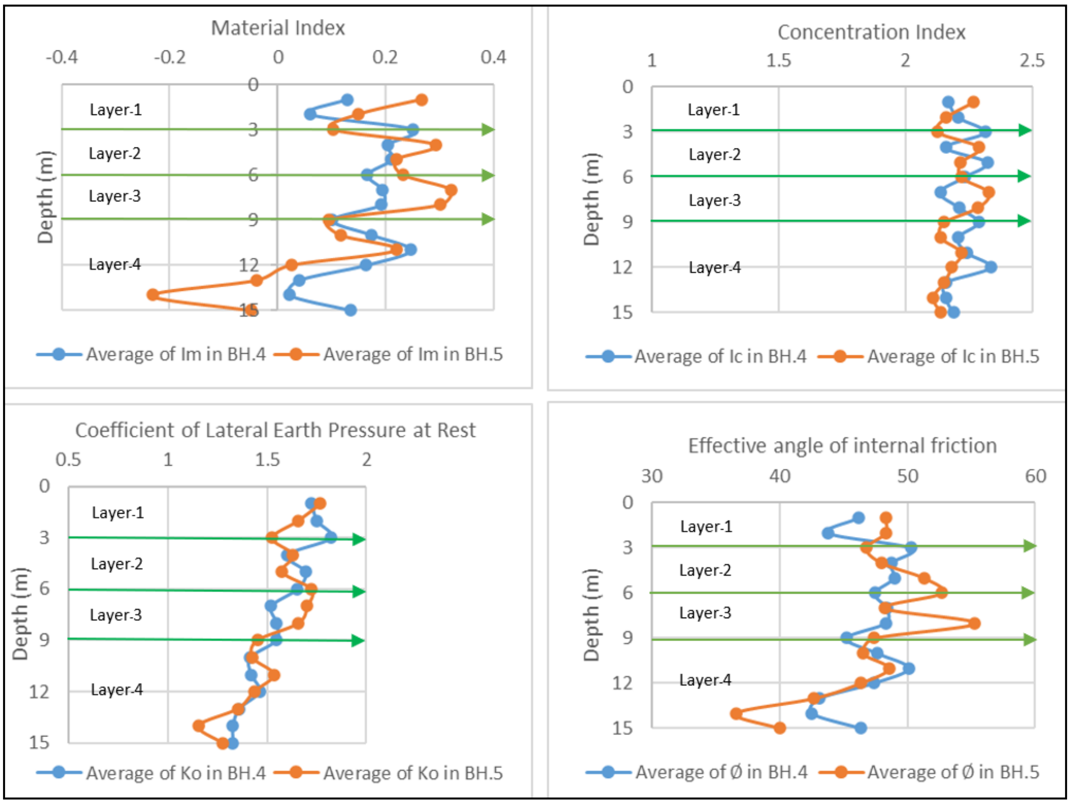


**Fig. 9.** Behavior of the average values of geotechnical properties of BH. 4 and BH. 5 with depth

## 6. Standard Penetration Test (SPT) and Ultimate Bearing Capacity ($Q_{ult}$)

The SPT mainly gives the subsoil foundations. Soil resistance for SPT depends on the overburden pressure, quality, and nature of the existing sand and the pore fluid pressure during the test. The SPT can be done for all types of soil and gives a good estimate of bearing capacity or shear strength values for sandy soil (cohesionless soil) and considers the value of shear resistance (Bowles, 1984). An empirical relationship between the N-value and shear velocity was expressed by Al-Khafaji (2010) for wet materials as equation 14.

$$Sin\ \emptyset = 2\ (V_s/V_p)^2 \tag{14}$$

The ultimate bearing capacity is an essential target of geotechnical properties because it indicates the soil's ability to accommodate the utilized loads. Thus, it gives the limits that should not be reached to avoid a structure failure. The $Q_{ult}$ was calculated by using the equations 15, 16 and 17 (Abdul Rahman, 1991).

Also, ultimate bearing capacity can be evaluated by using the standard penetration test or N-value for unconsolidated soil according to Parry's formula. Table (10) shows the approximate correlation between SPT, consistency, and Qult of clay and silt.

$$Q_{ult} = 2.348 \log V_s - 1.45 \quad (15)$$

$$Q_{ult} = 1 / [3.5 (V_p/240)^{2.38}] \quad (16)$$

$$Q_{ult} = 30\, N \text{ in (KPa) or } (KN/m^2) \quad (17)$$

**Table 10**. Approximate correlation between SPT consistency and $Q_{ult}$ of clay and silt (Terzaghi and Peck, 1967)

| SPT before injection (N-values) | Consistency | Ultimate Bearing Capacity | |
|---|---|---|---|
| | | **Ton/m²** | **kN/m²** |
| < 2 | Very soft | < 2.5 | < 25 |
| 2 – 4 | Soft | 2.5 – 5 | 25 – 50 |
| 4 – 8 | Medium stiff | 5 – 10 | 50 – 100 |
| 8 – 15 | Stiff | 10 – 20 | 100 – 200 |
| 16 – 30 | Very stiff | 20 – 40 | 200 – 400 |
| > 30 | Hard | > 40 | > 400 |

Table 7 shows the values of the $Q_{ult}$ in the studied site before and after injection they range between 2.68 and 14 T/m$^2$ (values of pink color) and 12.36 and 14 T/m$^2$, respectively. It clearly matches its individual SPT values from 3 to 15 m depth; as shown in Fig. 10. These values of $Q_{ult}$ refer to stiff layers and the soil site is allowable to bear light and medium weights. It indicates the heterogeneity of soil and differences in compaction in addition to the existence of water content, however, Qult after injection strongly enhanced the rigidity of the underlying soil in the site.

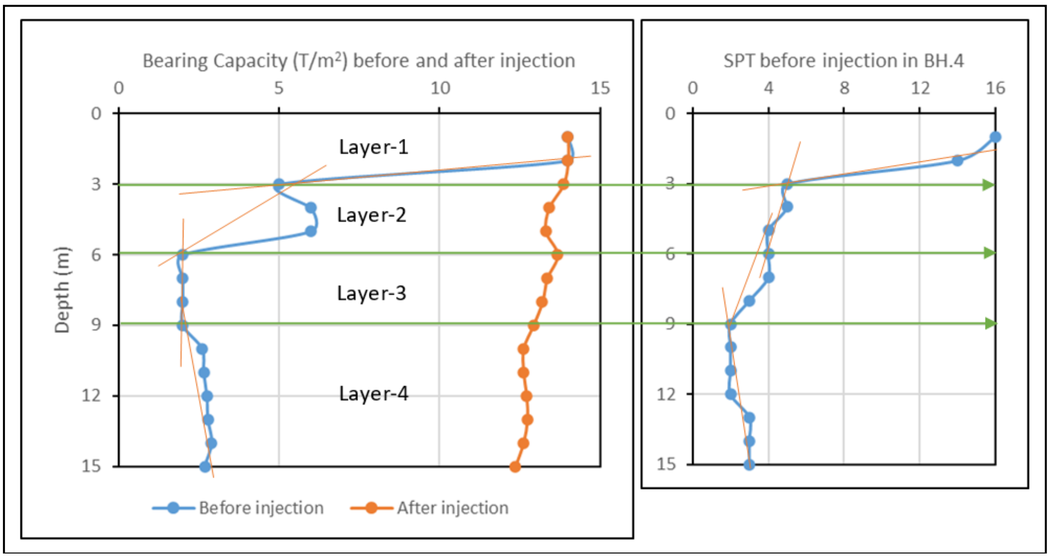


**Fig. 10.** Bearing Capacity before and after injection (treatment)

## 7. Safety Factor (Fs)

The safety factor is the ability of a structure capacity system to be applicable beyond its expected or intended load. Thus, to avoid engineering problems that may occur in the future. The safety factor is determined based on $V_p$ and $V_s$ and their ratio. The standard safety factor ranges between 1.5 and 5 regarding the ground characteristics and structural geometry. Besides, the $V_p/V_s$ ratio has interval variation of about 1.45 and 8 (Table 11). It is a high function of water saturation, porosity, crack intensity, and clay content (Keceli, 2000). It has been used as a lithological indicator in soil amplification projects, soil classification, and aquifer imaging (Carvalho et al., 2009). The soil bearing capacity is influenced by the presence of groundwater.

**Table 11.** The safety factor's values and Vp/vs ratios for soil and rocks (Khalil and Hanafy, 2008)

| Soil and rock type | $V_p$ (m/sec) | $V_s$ (m/sec) | ($V_p/V_s$) | Safety Factor (Fs) |
|---|---|---|---|---|
| Hard and massive rocks | 6000-4200 | 4000-2700 | 1.45-1.5 | 1.5 |
| Very Stiff | 4200-3000 | 2700-1500 | 1.5-2 | 1.5-2 |
| Stiff | 3000-2000 | 1500-700 | 2-3 | 2 |
| Moderate stiff but altered | 2000-1500 | 700-400 | 3-4 | 3 |
| Loose and soft | 1500-600 | 400-100 | 4-6 | 3-4 |
| Soft and saturated | <1300 | <100 | 5-8 | 4-5 |

The safety factors of the soils in the studied site range from 1.5 to 2 as shown in Table 11. However, the cover layer is considered a soft fill material with a thickness ranging from 0 to 1 m., which should be removed during the construction. The soil type of the investigated site is divided into four layers, the first one represents stiff to very stiff sandy silty clay at 2 to 3 m depth, the second layer consists of medium to stiff at (3 to 6) m depth, the third layer is stiff at (6 to 9) m depth and the fourth layer is soft silty clay at (9 to 15) m depths as illustrated in Table 12.

**Table 12.** shows Vp, Vs, VP/Vs, elastic modulus, and geotechnical properties of the studied site

| Depth (m) | Soil type | Averages of $V_p$ | $V_s$ | $V_p/V_s$ | Σ | μ (MPa) | E (MPa) | K (MPa) | $I_m$ | $I_c$ | $K_o$ | ø | $Q_{ult}$ after injection (Ton/m$^2$) | $F_s$ |
|---|---|---|---|---|---|---|---|---|---|---|---|---|---|---|
| 1 | Cover soil | | | | | | | | | | | | | |
| 2, 3 | stiff to very stiff sandy silty clay | 1227.8 | 752.1 | 1.63 | 0.21803 | 100281.5 | 244.31 | 184.16 | 0.1404 | 2.2015 | 1.688 | 47.31 | 13.93 | 1.5-2 |
| 4, 5, 6 | medium to stiff | 1210.8 | 748.5 | 1.62 | 0.1857 | 67959.6 | 241.74 | 208.92 | 0.2209 | 2.2393 | 1.646 | 49.53 | 13.46 | |
| 7 | stiff | 11 | 73 | 1.6 | 0.1 | 65 94 5.3 | 23 [illegible] | 20 | 0.2 | 2.2 | 1.5 71 | 48. 82 | 13. 16 | |

| | | | | | | | | | | | | | |
|---|---|---|---|---|---|---|---|---|---|---|---|---|---|
| 8 | | | | | | | | | | | | | |
| 9 | | | | | | | | | | | | | |
| 10 | | | | | | | | | | | | | |
| 11 12 13 14 15 | soft silty clay | 1177.4 | 704.9 | 1.67 | 0.24687 | 29709.8 | 221.881 | 150.91 | 0.0684 | 2.1848 | 1.374 | 44.83 | 12.60 |

## 8. Conclusions

The soil was investigated in a site for the construction of a hospital inside Basrah City to treat weak soil, where the soil was injected from 2 to 15 m depth by using improved cement and quick-hardening materials. The $V_p$ and $V_s$ were measured using Cross-hole seismic surveys. The velocity results showed that the subsurface soil can be divided into two zones due to the differences in velocity behavior, elastic, and geotechnical properties. The first zone extends at 2 to 9 m depth including three layers, and the second zone extends at (9 to 15) m depth. The soil within these depths is considered a homogeneous soil. The elasticity modules were calculated and the results showed that depths from 2-9 m differed from depths 9-15 m because they need more time to be solidified. However, Poisson's ratio values range between 0.18572 to 0.24687 in the studied site. It is believed that the soil type of the study area is clay when injected with cement materials. The geotechnical properties $I_m$, $I_C$, $K_o$ and Ø also gave results with little difference between these two zones. The geotechnical properties showed good soil parameters. Also, the result of the bearing capacity-$Q_{ult}$ before injection was a low stress of about < 5.2, but the results of the $Q_{ult}$ after injection was a high stress range between 12.36-14.06 Ton/m$^2$. This value refers to stiff layers and the soil site is allowed to bear light and medium weights.

The consistency layers of the study site are divided into four layers: the cover layer is a soft fill material from 0 to 1 m depth that should be removed during the construction. The first layer is stiff to very stiff sand silty clay at a depth of 2 to 3 m. The second layer consists of medium to stiff at a depth of 3 to 6 m, which is suitable for medium loads. The third layer is stiff at a depth of 6 to 9 m, which is suitable for medium and heavy foundations owing to the increase of the bulk density with depth; as a result of the compaction or load of the layers. Whereas, the fourth layer is soft silty clay at a depth of 9 to 15 m. It is clear from the obtained data that the layers from a depth of 3 to 15 meter are approximately close to the data of bore-holes of the study site.

## Acknowledgements

The authors would like to thank the anonymous reviewers for their insightful comments and suggestions. Moreover, we are particularly grateful to the Al-Mawal Company for their assistance in the field work including seismic surveys and engineering site investigations using their own geophysical instruments in the field.

## References

Abdel Rahman, M., 1991. Rock material competence assessed by seismic measurement with emphasis competence scale and application in some Urban areas in Yemen, E.G.S. proc. of 9th Annual Meeting, 9, 205-230.

Al-Amar, H.A.S., Al-Khalidi, A.A.L., 2018. Study of engineering properties by using downhole method for south Baghdad area in Iraq. International Journal of Civil Engineering and Technology, 9(9), 508–520.

Al-Amar, H.A.S., Al-Khalidi, A.A.L., 2023. Study of engineering properties by using downhole method for South Baghdad Area in Iraq. International Journal of Civil Engineering and Technology, 9, (9), 508-520.

Al-Amar, H.A.S., Al-Khalidi, A.A.L., Hadi, A.H., 2018. Assessment of soil banks of part from Shatt Al-Hilla in Al Hilla City/ Babylon Governorate. International Journal of Civil Engineering and Technology, 9(11), 2306–2315.

Al-Kafaji, A.J.M., 2004. The Use of Seismic Methods for Investigating Weak Zones and Geotechnical Evaluation of Al-Hussain Pure Water Site-Kerbala. M.Sc. Thesis, College of Science, University of Baghdad.

Al-Khafaji, A.J.M., 2010. Geophysical and Geotechnical Investigations of Soil Underneath the Foundation of Al-Abbas Holy Shrine Site in Karbala Governorate. M.Sc. Thesis, College of science, University of Baghdad (Unpublished).

Al-Khersan, E.H., Al-Khalidy, A.A., Al-Shimaree, A., 2012. Geophysical study for both Hilla-2 and Karbala-2 Gas Power Plants - Central Iraq with the assistance of the engineering information. International Journal of Emerging Technology and Advanced Engineering, 4, 568-587.

Al-Khersan, E.H., Hijab, B. R. and Baban, E.N., 2007. Paleomagnetic Study of Some Outcropping Rocks Northeastern Iraq and its Tectonic Applications. PhD. Thesis, College of Science, University of Baghdad (Unpublished).

Al-Sinawi, S.A., Khorshid, S.Z.A., Hamdi, F.A.I, 1990. Application of compressional and shear wave velocities in solving geotechnical problems associated with gypsiferous sediments in central Iraq. Iraqi Journal of Science, 13 (3), 591-610.

Al-Siyab, A., Al-Ansari, N., Al-Rawi, D., Al-Jassem, J., Al-Omari, F., Al-Sheikh, Z., 1982. Geology of Iraq. Dar Al Kutub Publishing House, Mosul, Iraq.

Ameen, N.N., 2006. Laboratory seismic study for some geotechnical properties of rocks for engineering purpose. M. Sc. Thesis, College of Science, University of Basra (Unpublished).

ASTM. D4428/D4428M–00. Standard test methods for cross-hole seismic testing.

Bowles, J.E., 1984. Physical and geotechnical properties of soil ($2^{nd}$ ed). Intonation student Edition, Mc-Graw Hill Japan Ltd. Tokyo, Japan.

Bowles, J.E., 1988. Foundation analysis and design ($4^{th}$ ed.). McGraw-Hill Book Company Limited, England.

Buday, T., Jassim, S.Z., 1987. The Regional Geology of Iraq: Tectonics, Magmatism and Metamorphism. In: Kassab, I.I. and Abbas, M.J., Eds., Geology of Iraq, Geologic Survey, Baghdad.

Carvalho, J., Dias, R., Pinto, C., Leote, J. and Mendes, V.L., 2009. SPT seismic hazard seismic refraction soil classification and geotechnical data applied to the soil microzoning of Western Algarve, Portugal. European Journal of Environmental and Engineering Geophysics, 5, 3- 14.

Craig, R.F., 2004. Craig's soil mechanics ($7^{th}$ ed.). Department of Civil Engineering, University of Dundee UK.

Crice, D., 2002. Borehole shear-wave surveys for engineering site investigations. Geostuff, Olson Engineering, INC.

Dobrin, M.B., 1976. Introduction to geophysical prospecting (3rd ed). McGraw-Hill publ. Co, New York.

Gupta, S., 2013. Cross-hole and Downhole Seismic Test. Workshop Cum Demo Session, Cengrs.

Hunt, R.E., 1986. Geotechnical Engineering Analysis and Evaluation. McGraw-Hill Book Co.

Hussien, N.A., Kareem, H.H., Al-Saad, H.T., Yousif, O.H., Al-Aabonaji, A., 1991. Shatt Al-Arab basic scientific studies. Publications of the Center for Marine Sciences, University of Basrah.

Jassim, S.Z., Goff, J., 2006. Geology of Iraq. Dolin and Museum, Prague, Chic Republic.

Jedi, Z.N., Al-Khalidy, A.A., 2023. Comparing the results of geotechnical tests with the well seismic survey to find the dynamic modulus of elasticity for the surface soil sections in Hilla City. Iraqi Geological Journal, 56 (1E), 228-233.

Keceli, A.D., 2000. The Determination of the presumptive bearing capacity by means of the seismic method. Jeofizik, 14, 1-2 (in Turkish).

Khafaji, S.J., Al-Ali, S.H., Al-Saad, H.A., 2010. Diagnosing and concentration in some feldspar sand sand deposits, southern Iraq. Basra Research Magazine, 36 (5), 12-34.

Khalil, M.H., Hanafy, S.M., 2008. Engineering application of seismic refraction method; a field example at Wadi Wardan, NE, Sinai, Egypt. Journal of Applied Geophysics 65 (3–4), 132-141.

Khorshid, S.Z., Al-Awsi, M., Al-Banna, A.S., 2014. Geotechnical evaluation to the soil of Tikrit University using seismic refraction method. Diyala Journal for Pure Sciences, 10 (2), 1-17.

Massarsch, K.R., 2007. The Practical Application of Seismic Testing in Geotechnical Engineering. Geotechnica et Mechanica studies, 29 (1-2), 121-135.

Menard, I., 2018. The Principles of Soil Mechanics. Callisto Reference.

Mohsain, A.F., Al-Khalidy, A.A.L., 2022. Geotechnical Assessment of Dar Al Salam Complex in Hilla City, Babylon Using the Seismic Refraction. Iraqi Geological Journal, 55(1F), 95–101.

Park, C.S., Lim, J.Y., Choi. C.L., Kong, B.C., Mok, Y.J., 2008. Recent development of borehole seismic tests. the 14th world conference on earthquake engineering, Beijing, China.

Saify, Z.M.J., Alkhalidy, A.A.L., 2023. Engineering, geophysical investigation of a multistory building, at Hilla, Iraq, Utilizing the MASW Method. Iraqi Geological Journal, 56(1), 217–227.

Stokoe, K., Santamarina, J., 2000. Seismic wave-based testing in geotechnical engineering. University of Texas, Austin, Texas, USA Georgia Institute of Technology, Atlanta, Georgia, USA.

Swain, R.J., 1962. Recent Techniques for determination of in-situ elastic properties and measurement of motion amplification in layered media. Geophysics, 28, 237-421.

Terzaghi, K., Peck, R.B., 1967. Soil mechanics in engineering practice (2nd ed.). John Wiley and Sons. Inc., New York.

Uyanik, O., 2010. Compressional and shear-wave velocity measurements in unconsolidated top-soil and comparison of the results. International Journal of the Physical Sciences, 5(7), 1034-1039.

Yilmaz, O., Eser, M., Berilgen, M., 2006. Seismic, geotechnical, and earthquake engineering site characterization. SEG Technical Program Expanded Abstracts.